EUROPEAN ORGANIZATION FOR NUCLEAR RESEARCH (CERN)

CERN-EP-2016-166
LHCb-PAPER-2016-017
21/07/2016

Measurement of the $B_s^0 \to J/\psi\,\eta$ lifetime

The LHCb collaboration†

This paper is dedicated to the memory of our friend and colleague Ailsa Sparkes.

Abstract

Using a data set corresponding to an integrated luminosity of $3\,\text{fb}^{-1}$, collected by the LHCb experiment in pp collisions at centre-of-mass energies of 7 and 8 TeV, the effective lifetime in the $B_s^0 \to J/\psi\,\eta$ decay mode, τ_{eff}, is measured to be

$$\tau_{\text{eff}} = 1.479 \pm 0.034\,(\text{stat}) \pm 0.011\,(\text{syst})\,\text{ps}.$$

Assuming CP conservation, τ_{eff} corresponds to the lifetime of the light B_s^0 mass eigenstate. This is the first measurement of the effective lifetime in this decay mode.

Submitted to Phys. Lett. B.

†Authors are listed at the end of this paper.

1 Introduction

Studies of $B_s^0-\overline{B}{}_s^0$ mixing provide important tests of the Standard Model (SM) of particle physics. In the SM, mixing occurs via box diagrams. Extensions to the SM may introduce additional *CP*-violating phases that alter the value of the $B_s^0-\overline{B}{}_s^0$ mixing weak phase, ϕ_s, from that of the SM [1]. The B_s^0 system exhibits a sizeable difference in the decay widths $\Gamma_{\rm L}$ and $\Gamma_{\rm H}$, where L and H refer to the light and heavy B_s^0 mass eigenstates, respectively. The effective lifetime, $\tau_{\rm eff}$, of a B_s^0 meson decay mode is measured by approximating the decay time distribution by a single exponential function. For final states that can be accessed by both B_s^0 and $\overline{B}{}_s^0$ mesons the effective lifetime depends on their *CP* components and is also sensitive to ϕ_s [2,3].

The golden channel to measure ϕ_s is the decay $B_s^0\to J/\psi\,\phi$ since it gives a clean signal and is relatively abundant. However, as there are two vector mesons in the final state, a time-dependent angular analysis is needed to disentangle the *CP*-even and *CP*-odd components. An alternative approach is to use *CP*-eigenstate modes, which contain either a scalar or pseudoscalar meson in the final state, such as $B_s^0\to J/\psi\,f_0(980)$ or $B_s^0\to J/\psi\,\eta^{(\prime)}$ decays. Although these decays are less copious they have the advantage that no angular analysis may be necessary.

In this analysis $\tau_{\rm eff}$ is determined for the *CP*-even $B_s^0\to J/\psi\,\eta$ decay mode. As ϕ_s is measured to be small [4,5] the mass eigenstates are also *CP* eigenstates to better than a permille and $\tau_{\rm eff}$ measured in $B_s^0\to J/\psi\,\eta$ decays is equal, to good approximation, to the lifetime of the light B_s^0 mass eigenstate, $\tau_{\rm L}=\Gamma_{\rm L}^{-1}$. In the SM $\tau_{\rm L}$ is predicted to be $1.43\pm0.03\,{\rm ps}$ [6]. Measurements of $\tau_{\rm L}$ have previously been reported by LHCb in the $B_s^0\to D_s^+D_s^-$ and $B_s^0\to K^+K^-$ decay modes [7,8]. The latter is dominated by penguin diagrams, which could arise within and beyond the SM and gives rise to direct *CP* violation in the $B_s^0\to K^+K^-$ decay. This then leads to a different $\tau_{\rm eff}$, when compared to measurements in the $B_s^0\to D_s^+D_s^-$ and $B_s^0\to J/\psi\,\eta$ decays which are mediated by tree diagrams. Improved precision on the effective lifetimes $\tau_{\rm L}$ and $\tau_{\rm H}$ will enable more stringent tests of the consistency between direct measurements of the decay width difference $\Delta\Gamma_s=\Gamma_{\rm L}-\Gamma_{\rm H}$ and ϕ_s measured in $B_s^0\to J/\psi\,\phi$ decays and those inferred using effective lifetimes.

The measurement of the effective $B_s^0\to J/\psi\,\eta$ lifetime presented in this Letter uses 3 $\rm fb^{-1}$ of data collected in *pp* collisions at centre-of-mass energies of 7 TeV and 8 TeV during 2011 and 2012 using the LHCb detector. The J/ψ meson is reconstructed via the dimuon decay mode and the η meson via the diphoton decay mode.

2 Detector and simulation

The LHCb detector [9,10] is a single-arm forward spectrometer covering the pseudorapidity range $2<\eta<5$, designed for the study of particles containing b or c quarks. The detector includes a high-precision tracking system consisting of a silicon-strip vertex detector surrounding the *pp* interaction region, a large-area silicon-strip detector (TT) located upstream of a dipole magnet with a bending power of about $4\,{\rm Tm}$, and three stations of silicon-strip detectors and straw drift tubes placed downstream of the magnet. The tracking system provides a measurement of momentum, p, of charged particles with a relative uncertainty that varies from 0.5 % at low momentum to 1.0 % at $200\,{\rm GeV}/c$.

Large samples of $J/\psi \to \mu^+\mu^-$ and $B^+ \to J/\psi K^+$ and decays, collected concurrently with the data set used here, were used to calibrate the momentum scale of the spectrometer to a precision of 0.03 % [11]. The minimum distance of a track to a primary vertex (PV), the impact parameter (IP), is measured with a resolution of $(15 + 29/p_{\mathrm{T}})\,\mu\mathrm{m}$, where p_{T} is the component of the momentum transverse to the beam, in GeV/c.

Different types of charged hadrons are distinguished using information from two ring-imaging Cherenkov detectors. Photons, electrons and hadrons are identified by a calorimeter system consisting of scintillating-pad and preshower detectors, an electromagnetic calorimeter and a hadronic calorimeter. The calorimeter response is calibrated using samples of $\pi^0 \to \gamma\gamma$ decays. For this analysis a further calibration was made using the decay $\eta \to \gamma\gamma$, which results in a precision of 0.07 % on the neutral energy scale. Muons are identified by a system composed of alternating layers of iron and multiwire proportional chambers.

The online event selection is performed by a trigger [12], which consists of a hardware stage, based on information from the calorimeter and muon systems, followed by a software stage, where a full event reconstruction is made. Candidate events are required to pass the hardware trigger, which selects muon and dimuon candidates with high p_{T} based upon muon system information. The subsequent software trigger is composed of two stages. The first performs a partial event reconstruction and requires events to have two well-identified oppositely charged muons with an invariant mass larger than 2.7 GeV/c^2. The second stage performs a full event reconstruction. Events are retained for further processing if they contain a $J/\psi \to \mu^+\mu^-$ candidate that is significantly displaced from all primary vertices. This introduces a non-uniform efficiency as a function of decay time.

Simulated pp collisions are generated using Pythia [13] with a specific LHCb configuration [14]. Decays of hadronic particles are described by EvtGen [15], in which final-state radiation is generated using Photos [16]. The interaction of the generated particles with the detector, and its response, are implemented using the Geant4 toolkit [17] as described in Ref. [18].

3 Selection

A two-step procedure is used to select $B_s^0 \to J/\psi\,\eta$ decay candidates. First, loose selection criteria are applied that reduce background significantly whilst retaining high signal efficiency. Subsequently, a multivariate selection (MVA) is used to reduce further the combinatorial background. This is optimized using pseudoexperiments to obtain the best precision on the measured B_s^0 lifetime.

The selection starts from a pair of oppositely charged particles, identified as muons, that form a common decay vertex. Combinatorial background is suppressed by requiring the muon candidates to be significantly displaced from all PVs in the event. To ensure a high reconstruction efficiency the muon candidates are required to have a pseudorapidity between 2.0 and 4.5. The invariant mass of the dimuon candidate must be within 50 MeV/c^2 of the known J/ψ mass [19]. The decay vertex is required to be well separated from the reconstructed PV of the proton-proton interaction by requiring the J/ψ decay length divided by its uncertainty to be greater than three.

Photons are selected from neutral clusters reconstructed in the electromagnetic calorimeter [10] that have a transverse energy in excess of 300 MeV and a confidence level to be a photon, $\mathcal{P}_\gamma$, greater than 0.009. The latter requirement has an efficiency of 98 % for the signal whilst removing 23 % of the combinatorial background. To suppress combinatorial background, any pair of photons in the event that have an invariant mass within 25 MeV/c^2 of the known π^0 meson mass [19] are rejected.

Candidate $\eta \to \gamma\gamma$ decays are selected from diphoton combinations with an invariant mass within 70 MeV/c^2 of the known η mass [19] and with a transverse momentum larger than 2 GeV/c. The decay angle between the photon momentum in the η rest frame and the direction of Lorentz boost from the laboratory frame to the η rest frame, θ^*_η, is required to satisfy $\left|\cos\theta^*_\eta\right| < 0.8$.

The J/ψ and η candidates are combined to form candidate $B^0_{(s)}$ mesons. The average number of PVs in each event is two. When multiple PVs are reconstructed, the one with the minimum $\chi^2_{\rm IP}$ to the $B^0_{(s)}$ candidate is chosen [1]. A kinematic fit is performed to improve the invariant mass resolution [20]. In this fit the momentum vector of the $B^0_{(s)}$ candidate is constrained to point to the PV and the intermediate resonance masses are constrained to their known values. The reduced χ^2 of this fit, $\chi^2/\rm ndf$, is required to be less than five. The measured $B^0_{(s)}$ decay time must be larger than 0.3 ps and less than 10 ps. If more than one PV is reconstructed in an event the properties of the unassociated vertices are studied. Any candidate for which there is a second PV which can be matched to it with reasonable quality is discarded. This requirement slightly distorts the decay time distribution but reduces background due to incorrect association of the $B^0_{(s)}$ candidate to a PV. Finally, as in Ref. [21], the position of the PV along the beam-line is required to be within 10 cm of the nominal interaction point, where the standard deviation of this variable is approximately 5 cm. This criterion leads to a 10 % reduction in signal yield but defines a fiducial region where the reconstruction efficiency is uniform.

The second step of the selection process is based on a neural network [22], which is trained using the simulated signal sample and the high-mass sideband of the data for background. Seven variables that show good agreement between data and simulation and that do not bias the $B^0_{(s)}$ decay time distribution are used to train the neural net: the $\chi^2/\rm ndf$ of the kinematic fit; the $p_{\rm T}$ of the $B^0_{(s)}$ and η mesons; the minimum $p_{\rm T}$ of the two photons; $\left|\cos\theta^*_\eta\right|$; the minimum $\mathcal{P}_\gamma$ of the two photons and the hit multiplicity in the TT sub-detector.

The requirement on the MVA output was chosen to minimize the statistical uncertainty on the fitted $\tau_{\rm eff}$ using a sample of 100 pseudoexperiments. The chosen value removes 94 % of background candidates whilst retaining 69 % of the signal candidates. After applying these requirements 2 % of events contain multiple candidates from which only one, chosen at random, is kept.

4 Fit model

The effective lifetime is determined by performing a two-dimensional maximum likelihood fit to the unbinned distributions of the $B^0_{(s)}$ candidate invariant mass and decay time. The fit model has four components: the $B^0_s \to J/\psi\,\eta$ signal, background from the $B^0 \to J/\psi\,\eta$ decay, background from partially reconstructed $B^0_s \to J/\psi\,\eta X$ decays, and combinatorial background.

[1]The quantity $\chi^2_{\rm IP}$ is defined as the difference between the χ^2 of the PV reconstructed with and without the considered particle.

In the fit, the decay-time distribution of each component is convolved with a Gaussian resolution function whose width is fixed to the standard deviation of the decay-time resolution in simulated data. A decay-time acceptance function accounts for the dependence of the signal efficiency on several effects. The overall acceptance, A_{tot}, is the product of the selection (A_{sel}), trigger (A_{trig}) and vertex (A_{β}) acceptance functions, determined as described below. The dominant effect, A_{sel}, is due to the selection requirements, in particular the cut on the displacement of the muons from the PV. This is studied using simulation and parameterised with the form

$$A_{\text{sel}} = \frac{1 - c_0 t}{1 + (c_1 t)^{-c_2}},$$

where t is the decay time, and c_0, c_1 and c_2 are parameters determined from the simulation. In the second level of the software trigger a cut is applied on the decay length significance of the J/ψ candidate, which biases the decay time distribution. The trigger efficiency, A_{trig}, is measured separately for the 2011 and 2012 dataset using events that are selected by a dedicated trigger in which this requirement is removed. The resulting acceptance shape is parameterised in bins of decay time. Finally, the reconstruction efficiency of the vertex detector decreases as the distance of closest approach of the decay products to the pp beam-line increases. This effect is studied using $B^+ \to J/\psi K^+$ decays where the kaon is reconstructed without using vertex detector information [21] and parameterised with the form

$$A_{\beta} = 1 - \beta t - \gamma t^2,$$

where the parameters β and γ are determined separately for the 2011 and 2012 data. Figure 1 shows the acceptance curve obtained for the 2011 and 2012 dataset.

The invariant mass distribution for the $B^0_s \to J/\psi \eta$ signal is parameterized by a Student's t-distribution. The Bukin [23] and JohnsonSU [24] functions are considered for systematic variations. In the fit to the data, the shape parameters of this distribution are fixed to the simulation values. The decay time distribution for this component is modelled with an exponential function convolved with the detector resolution and multiplied by the detector acceptance, as discussed above.

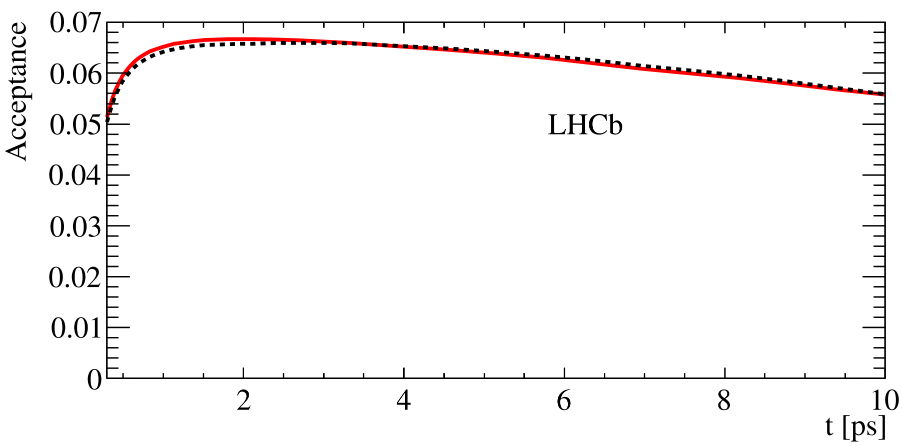

Figure 1: Acceptance function for 2011 data (black dashed line) and 2012 data (solid red).

The second component in the fit accounts for the $B^0 \to J/\psi\eta$ decay. As the invariant mass resolution is approximately $48\,\mathrm{MeV}/c^2$ this overlaps with the B_s^0 signal mode. Its mass distribution is modelled, analogously to the B_s^0 component, with a Student's t-distribution, with resolution parameters fixed to values determined in the simulation. The mass difference between the B_s^0 and B^0 mesons, and the B^0 lifetime, are fixed to their known values: $m(B_s^0) - (B^0) = 87.29 \pm 0.26\,\mathrm{MeV}/c^2$ [25] and $\tau(B^0) = 1.519 \pm 0.005\,\mathrm{ps}$ [19]. The relative yield of the B_s^0 and B^0 components, f_r, is fixed to $(7.3 \pm 0.8)\,\%$ calculated from the average of the branching fractions measurements made by the Belle [26, 27] and LHCb collaborations [28], and the measured fragmentation fractions [29–31].

Combinatorial background is modelled by a linear function in mass and a double exponential in decay time. In the fit to the data the lifetime of the shorter lived component is fixed to the value found in the fit to the sideband. As a systematic variation of the mass model, an exponential function is considered. An additional background component arises at masses below $5100\,\mathrm{MeV}/c^2$ due to partially reconstructed $B_s^0 \to J/\psi\eta X$ decays. This is modelled by a Novosibirsk function [32] in mass and an exponential in time. All parameters of this component apart from the yield are fixed to the simulation values in the fit to the data.

The fit has eight free parameters: the yield of the $B_s^0 \to J/\psi\eta$ component ($N^{B_s^0}$), the combinatorial background yield (N^{comb}), the partially reconstructed background yield (N^{partial}), the B_s^0 mass, the lifetime of the signal component (τ_{eff}), the coefficient of the combinatorial background component in mass (a_{back}), the longer lived background lifetime (τ_{back}) and the fraction of the short-lived background (f_{back}). Independent fits are performed for the 2011 and 2012 data and a weighted average of the two lifetime values is made.

5 Results

Figure 2 shows the fit projections in mass and decay time for the 2011 and 2012 data. The corresponding fit results are summarized in Table 1. The average of the fitted values of τ_{eff} is

$$\tau_{\mathrm{eff}} = 1.479 \pm 0.034\,\mathrm{ps},$$

where the uncertainty is statistical.

The dominant source of systematic uncertainty is due to the modelling of the time acceptance of the detector. The procedure used to determine the decay time acceptance has been validated using the simulation with a statistical precision of 10 fs. The statistical and systematic uncertainties on A_β are evaluated by repeating the fit and varying the parameterisation within its uncertainties. The statistical uncertainty on A_{trig} is propagated by generating an ensemble of histograms with each bin varied within its statistical uncertainty. Systematic uncertainties on A_{trig} are estimated to be small by varying the binning of the histogram and considering an alternative analytic form. Possible biases in the time acceptance due to the MVA selection are evaluated to be 1.7 fs.

The influence of the decay time resolution is estimated by increasing its value from 51 to 70 fs and found to be negligible. The impact of the uncertainties in f_r, the $B_s^0 - B^0$ mass splitting, and the B^0 lifetime are evaluated by repeating the fit procedure varying these parameters within their quoted uncertainties.

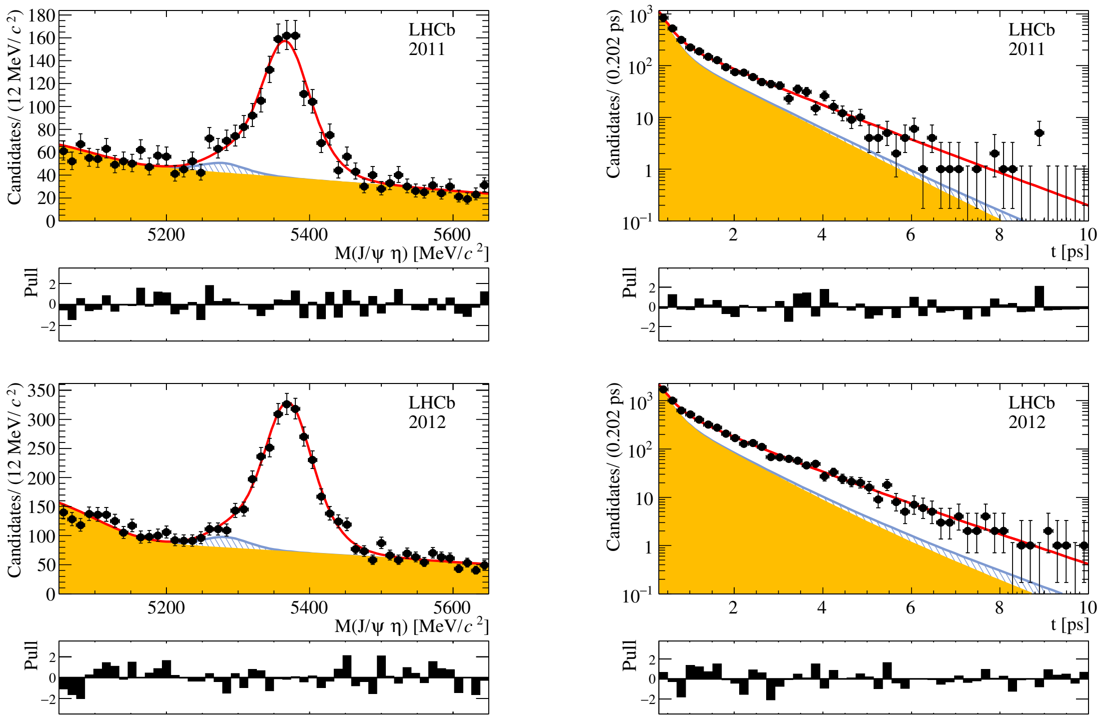

Figure 2: Mass and decay time distributions for the 2011 dataset (top row) and 2012 dataset (bottom row). The fit model described in the text is superimposed (red line). The sum of the partially reconstructed and combinatorial background is shown (solid yellow) and the B^0 component (open blue). The pull, *i.e.* the difference between the observed and fitted value divided by the uncertainty, is shown below each of the plots.

Further uncertainties arise from the modelling of the time distributions of the background components. In the default fit the lifetime of the short-lived component is fixed to the value found in a fit to the mass sideband. Removing this constraint changes the result by 4 fs, which is assigned as a systematic uncertainty. The uncertainty due to the fixed lifetime of the partially reconstructed component is found to be negligible.

Uncertainties arising from the modelling of the signal and background mass distributions are evaluated using the discrete profiling method described in Ref. [33] and found to be negligible. Further small uncertainties arise due to the limited knowledge of the length scale of the detector along the beam axis, the charged particle momentum scale and the neutral particle energy scale.

The stability of the result has been tested against a number of possible variations, such as the requirement on the IP of the muons, the MVA requirement and analysing the sample according to the number of reconstructed PVs. No significant change in the final result is found and hence no further systematic uncertainty is assigned.

All the uncertainties are summarized in Table 2. Adding them in quadrature leads to a total systematic uncertainty of 11.1 fs which is dominated by the size of the simulation sample used to determine the acceptance and to validate the analysis procedure.

Table 1: Parameters of the fit to $B^0_{(s)} \to J/\psi\eta$ candidates for the 2011 and 2012 datasets. Uncertainties are statistical only.

Fit parameter	Fitted value	
	2011	2012
$N^{B^0_s}$	960 ± 42	2061 ± 60
$m_{B^0_s}$ [MeV/c^2]	5365.6 ± 1.8	5369.6 ± 1.3
τ_{eff} [ps]	1.485 ± 0.060	1.476 ± 0.041
N^{comb}	1898 ± 64	3643 ± 89
N^{partial}	81 ± 26	345 ± 39
a_{back}	-0.37 ± 0.05	-0.31 ± 0.03
f_{back}	0.52 ± 0.03	0.49 ± 0.02
τ_{back} [ps]	0.97 ± 0.06	0.82 ± 0.04

Table 2: Systematic uncertainties on the lifetime measurement. Uncertainties less than 0.1 fs are indicated by a dash.

Source	Uncertainty [fs]
Simulation validation	10.0
A_β (stat)	2.0
A_β (syst)	0.1
A_{trig} (stat)	0.6
A_{trig} (syst)	0.6
MVA	1.7
Time resolution	–
f_r	1.2
$B^0_s - B^0$ mass difference	–
B^0 lifetime	0.2
Releasing τ_{back}	4.0
Varying τ_{partial}	–
Mass model	–
Momentum scale	–
z-scale	0.3
Total	11.1

6 Summary

Using data collected by LHCb, the effective lifetime in the $B^0_s \to J/\psi\eta$ decay mode is measured to be

$$\tau_{\text{eff}} = 1.479 \pm 0.034 \text{ (stat)} \pm 0.011 \text{ (syst) ps}.$$

In the limit of CP conservation, τ_{eff} is equal to the lifetime of the light B_s^0 mass eigenstate τ_L. The present measurement is consistent with, and has similar precision to, the effective lifetime determined using the $B_s^0 \to D_s^+ D_s^-$ decay mode [7], $\tau_{\text{eff}}(D_s^+ D_s^-) = 1.379 \pm 0.026\,(\text{stat}) \pm 0.017\,(\text{syst})$ ps and also with the value measured in the $B_s^0 \to K^+ K^-$ mode [8], $\tau_{\text{eff}}(K^+ K^-) = 1.407 \pm 0.016\,(\text{stat}) \pm 0.007\,(\text{syst})$ ps where penguin diagrams are expected to be more important. Averaging the tree level measurements gives $\tau_{\text{eff}} = 1.42 \pm 0.02$ ps in good agreement with the expectations of the Standard Model [6], $\tau_{\text{L}} = 1.43 \pm 0.03$ ps and the value quoted by HFAG [34] from measurements made in the $B_s^0 \to J/\psi\,\phi$ mode, $\tau_{\text{L}} = 1.420 \pm 0.006$ ps. The values from these different measurements are compared in Fig. 3.

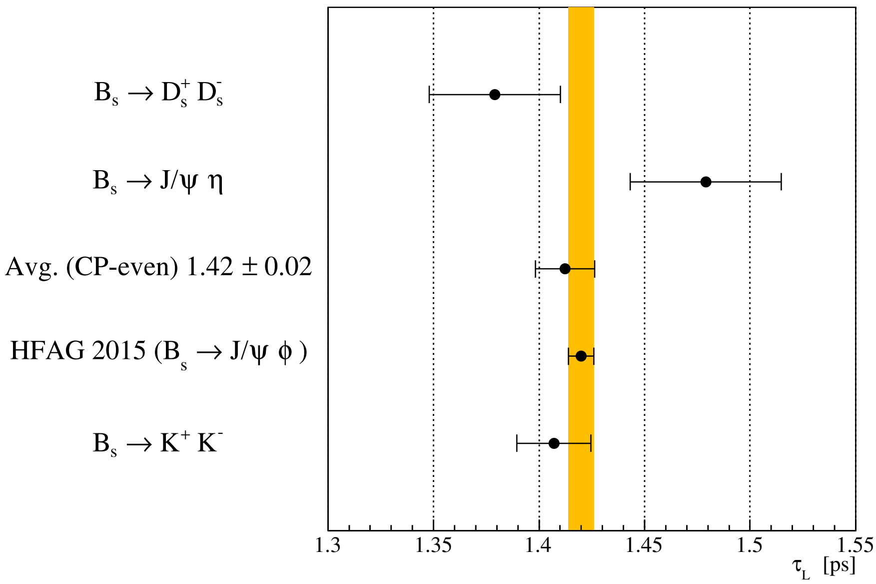

Figure 3: Summary of measurements of τ_{L}. The yellow band corresponds to the 2015 HFAG central value and uncertainty.

Acknowledgements

We express our gratitude to our colleagues in the CERN accelerator departments for the excellent performance of the LHC. We thank the technical and administrative staff at the LHCb institutes. We acknowledge support from CERN and from the national agencies: CAPES, CNPq, FAPERJ and FINEP (Brazil); NSFC (China); CNRS/IN2P3 (France); BMBF, DFG and MPG (Germany); INFN (Italy); FOM and NWO (The Netherlands); MNiSW and NCN (Poland); MEN/IFA (Romania); MinES and FANO (Russia); MinECo (Spain); SNSF and SER (Switzerland); NASU (Ukraine); STFC (United Kingdom); NSF (USA). We acknowledge the computing resources that are provided by CERN, IN2P3 (France), KIT and DESY (Germany), INFN (Italy), SURF (The Netherlands), PIC (Spain), GridPP (United Kingdom), RRCKI and Yandex LLC (Russia), CSCS (Switzerland), IFIN-HH (Romania), CBPF (Brazil), PL-GRID (Poland) and OSC (USA). We are indebted to the communities behind the multiple open source software packages on which we depend. Individual groups or members have received support from AvH Foundation (Germany), EPLANET, Marie Skłodowska-Curie Actions and ERC (European Union), Conseil Général de Haute-Savoie, Labex ENIGMASS and OCEVU, Région Auvergne (France), RFBR and Yandex LLC (Russia), GVA, XuntaGal and GENCAT (Spain), Herchel Smith Fund, The Royal Society, Royal Commission for the Exhibition of 1851 and the Leverhulme Trust (United Kingdom).

References

[1] LHCb collaboration, R. Aaij *et al.* , and A. Bharucha *et al.*, *Implications of LHCb measurements and future prospects*, Eur. Phys. J. **C73** (2013) 2373, arXiv:1208.3355.

[2] R. Fleischer and R. Knegjens, *Effective lifetimes of B_s decays and their constraints on the B_s^0-$\overline{B}_s^0$ mixing parameters*, Eur. Phys. J. **C71** (2011) 1789, arXiv:1109.5115.

[3] R. Fleischer, R. Knegjens, and G. Ricciardi, *Exploring CP violation and η-η' mixing with the $B_{s,d}^0 \to J/\psi\,\eta^{(\prime)}$ systems*, Eur. Phys. J. **C71** (2011) 1798, arXiv:1110.5490.

[4] LHCb collaboration, R. Aaij *et al.*, *Precision measurement of CP violation in $B_s^0 \to J/\psi\,K^+K^-$ decays*, Phys. Rev. Lett. **114** (2015) 041801, arXiv:1411.3104.

[5] LHCb collaboration, R. Aaij *et al.*, *Measurement of the CP-violating phase ϕ_s in $\overline{B}_s^0 \to J/\psi\,\pi^+\pi^-$ decays*, Phys. Lett. **B736** (2014) 186, arXiv:1405.4140.

[6] A. Lenz, *Theoretical update of B-Mixing and lifetimes*, in *2012 Electroweak Interactions and Unified Theories*, Moriond, 2012. arXiv:1205.1444.

[7] LHCb collaboration, R. Aaij *et al.*, *Measurement of the $\overline{B}_s^0 \to D_s^- D_s^+$ and $\overline{B}_s^0 \to D^- D_s^+$ effective lifetimes*, Phys. Rev. Lett. **112** (2014) 111802, arXiv:1312.1217.

[8] LHCb collaboration, R. Aaij *et al.*, *Effective lifetime measurements in the $B_s^0 \to K^+K^-$, $B^0 \to K^+\pi^-$ and $B_s^0 \to \pi^+K^-$ decays*, Phys. Lett. **B736** (2014) 446, arXiv:1406.7204.

[9] LHCb collaboration, A. A. Alves Jr. *et al.*, *The LHCb detector at the LHC*, JINST **3** (2008) S08005.

[10] LHCb collaboration, R. Aaij *et al.*, *LHCb detector performance*, Int. J. Mod. Phys. **A30** (2015) 1530022, arXiv:1412.6352.

[11] LHCb collaboration, R. Aaij *et al.*, *Measurements of the Λ_b^0, Ξ_b^-, and Ω_b^- baryon masses*, Phys. Rev. Lett. **110** (2013) 182001, arXiv:1302.1072.

[12] R. Aaij *et al.*, *The LHCb trigger and its performance in 2011*, JINST **8** (2013) P04022, arXiv:1211.3055.

[13] T. Sjöstrand, S. Mrenna, and P. Skands, *PYTHIA 6.4 physics and manual*, JHEP **05** (2006) 026, arXiv:hep-ph/0603175; T. Sjöstrand, S. Mrenna, and P. Skands, *A brief introduction to PYTHIA 8.1*, Comput. Phys. Commun. **178** (2008) 852, arXiv:0710.3820.

[14] I. Belyaev *et al.*, *Handling of the generation of primary events in Gauss, the LHCb simulation framework*, J. Phys. Conf. Ser. **331** (2011) 032047.

[15] D. J. Lange, *The EvtGen particle decay simulation package*, Nucl. Instrum. Meth. **A462** (2001) 152.

[16] P. Golonka and Z. Was, *PHOTOS Monte Carlo: A precision tool for QED corrections in Z and W decays*, Eur. Phys. J. **C45** (2006) 97, arXiv:hep-ph/0506026.

[17] Geant4 collaboration, J. Allison *et al.*, *Geant4 developments and applications*, IEEE Trans. Nucl. Sci. **53** (2006) 270; Geant4 collaboration, S. Agostinelli *et al.*, *Geant4: A simulation toolkit*, Nucl. Instrum. Meth. **A506** (2003) 250.

[18] M. Clemencic *et al.*, *The LHCb simulation application, Gauss: Design, evolution and experience*, J. Phys. Conf. Ser. **331** (2011) 032023.

[19] Particle Data Group, K. A. Olive *et al.*, *Review of particle physics*, Chin. Phys. **C38** (2014) 090001, and 2015 update.

[20] W. D. Hulsbergen, *Decay chain fitting with a Kalman filter*, Nucl. Instrum. Meth. **A552** (2005) 566, `arXiv:physics/0503191`.

[21] LHCb collaboration, R. Aaij *et al.*, *Measurements of the B^+, B^0, B^0_s meson and Λ^0_b baryon lifetimes*, JHEP **04** (2014) 114, `arXiv:1402.2554`.

[22] A. Hoecker *et al.*, *TMVA: Toolkit for multivariate data analysis*, PoS **ACAT** (2007) 040, `arXiv:physics/0703039`.

[23] BABAR collaboration, J. P. Lees *et al.*, *Branching fraction measurements of the color-suppressed decays $\overline{B}^0 \to D^{(*)0}\pi^0$, $D^{(*)0}\eta$, $D^{(*)0}\omega$, and $D^{(*)0}\eta'$ and measurement of the polarization in the decay $\overline{B}^0 \to D^{*0}\omega$*, Phys. Rev. **D84** (2011) 112007, `arXiv:1107.5751`, [Erratum: Phys. Rev.D87,039901(2013)].

[24] N. L. Johnson, *Systems of frequency curves generated by methods of translation*, Biometrika **36** (1949), no. 1-2 149.

[25] LHCb collaboration, R. Aaij *et al.*, *Observation of the decay $\overline{B}^0_s \to \psi(2S)K^+\pi^-$*, Phys. Lett. **B747** (2015) 484, `arXiv:1503.07112`.

[26] Belle collaboration, M. C. Chang *et al.*, *Observation of the decay $B^0 \to J/\psi\,\eta$*, Phys. Rev. Lett. **98** (2007) 131803, `arXiv:hep-ex/0609047`.

[27] Belle collaboration, M. C. Chang *et al.*, *Measurement of $B^0 \to J/\psi\,\eta^{(\prime)}$ and constraint on the $\eta - \eta'$ mixing angle*, Phys. Rev. **D85** (2012) 091102, `arXiv:1203.3399`.

[28] LHCb collaboration, R. Aaij *et al.*, *Study of η–η' mixing from measurement of $B^0_{(s)} \to J/\psi\,\eta^{(\prime)}$ decay rates*, JHEP **01** (2015) 024, `arXiv:1411.0943`.

[29] LHCb collaboration, R. Aaij *et al.*, *Measurement of b hadron production fractions in 7 TeV pp collisions*, Phys. Rev. **D85** (2012) 032008, `arXiv:1111.2357`.

[30] LHCb collaboration, R. Aaij *et al.*, *Measurement of the fragmentation fraction ratio f_s/f_d and its dependence on B meson kinematics*, JHEP **04** (2013) 001, `arXiv:1301.5286`.

[31] LHCb collaboration, *Updated average f_s/f_d b-hadron production fraction ratio for* 7 TeV *pp collisions*, LHCb-CONF-2013-011.

[32] Belle collaboration, H. Ikeda *et al.*, *A detailed test of the CsI(Tl) calorimeter for BELLE with photon beams of energy between 20-MeV and 5.4-GeV*, Nucl. Instrum. Meth. **A441** (2000) 401.

[33] P. D. Dauncey *et al.*, *Handling uncertainties in background shapes: the discrete profiling method*, JINST **10** (2015) P04015, arXiv:1408.6865.

[34] Heavy Flavor Averaging Group, Y. Amhis *et al.*, *Averages of b-hadron, c-hadron, and τ-lepton properties as of summer 2014*, arXiv:1412.7515, updated results and plots available at http://www.slac.stanford.edu/xorg/hfag/.

LHCb collaboration

R. Aaij[39], B. Adeva[38], M. Adinolfi[47], Z. Ajaltouni[5], S. Akar[6], J. Albrecht[10], F. Alessio[39], M. Alexander[52], S. Ali[42], G. Alkhazov[31], P. Alvarez Cartelle[54], A.A. Alves Jr[58], S. Amato[2], S. Amerio[23], Y. Amhis[7], L. An[40], L. Anderlini[18], G. Andreassi[40], M. Andreotti[17,g], J.E. Andrews[59], R.B. Appleby[55], O. Aquines Gutierrez[11], F. Archilli[1], P. d'Argent[12], J. Arnau Romeu[6], A. Artamonov[36], M. Artuso[60], E. Aslanides[6], G. Auriemma[26], M. Baalouch[5], I. Babuschkin[55], S. Bachmann[12], J.J. Back[49], A. Badalov[37], C. Baesso[61], W. Baldini[17], R.J. Barlow[55], C. Barschel[39], S. Barsuk[7], W. Barter[39], V. Batozskaya[29], B. Batsukh[60], V. Battista[40], A. Bay[40], L. Beaucourt[4], J. Beddow[52], F. Bedeschi[24], I. Bediaga[1], L.J. Bel[42], V. Bellee[40], N. Belloli[21,i], K. Belous[36], I. Belyaev[32], E. Ben-Haim[8], G. Bencivenni[19], S. Benson[39], J. Benton[47], A. Berezhnoy[33], R. Bernet[41], A. Bertolin[23], F. Betti[15], M.-O. Bettler[39], M. van Beuzekom[42], S. Bifani[46], P. Billoir[8], T. Bird[55], A. Birnkraut[10], A. Bitadze[55], A. Bizzeti[18,u], T. Blake[49], F. Blanc[40], J. Blouw[11], S. Blusk[60], V. Bocci[26], T. Boettcher[57], A. Bondar[35], N. Bondar[31,39], W. Bonivento[16], A. Borgheresi[21,i], S. Borghi[55], M. Borisyak[67], M. Borsato[38], F. Bossu[7], M. Boubdir[9], T.J.V. Bowcock[53], E. Bowen[41], C. Bozzi[17,39], S. Braun[12], M. Britsch[12], T. Britton[60], J. Brodzicka[55], E. Buchanan[47], C. Burr[55], A. Bursche[2], J. Buytaert[39], S. Cadeddu[16], R. Calabrese[17,g], M. Calvi[21,i], M. Calvo Gomez[37,m], P. Campana[19], D. Campora Perez[39], L. Capriotti[55], A. Carbone[15,e], G. Carboni[25,j], R. Cardinale[20,h], A. Cardini[16], P. Carniti[21,i], L. Carson[51], K. Carvalho Akiba[2], G. Casse[53], L. Cassina[21,i], L. Castillo Garcia[40], M. Cattaneo[39], Ch. Cauet[10], G. Cavallero[20], R. Cenci[24,t], M. Charles[8], Ph. Charpentier[39], G. Chatzikonstantinidis[46], M. Chefdeville[4], S. Chen[55], S.-F. Cheung[56], V. Chobanova[38], M. Chrzaszcz[41,27], X. Cid Vidal[38], G. Ciezarek[42], P.E.L. Clarke[51], M. Clemencic[39], H.V. Cliff[48], J. Closier[39], V. Coco[58], J. Cogan[6], E. Cogneras[5], V. Cogoni[16,39,f], L. Cojocariu[30], G. Collazuol[23,o], P. Collins[39], A. Comerma-Montells[12], A. Contu[39], A. Cook[47], S. Coquereau[8], G. Corti[39], M. Corvo[17,g], C.M. Costa Sobral[49], B. Couturier[39], G.A. Cowan[51], D.C. Craik[51], A. Crocombe[49], M. Cruz Torres[61], S. Cunliffe[54], R. Currie[54], C. D'Ambrosio[39], E. Dall'Occo[42], J. Dalseno[47], P.N.Y. David[42], A. Davis[58], O. De Aguiar Francisco[2], K. De Bruyn[6], S. De Capua[55], M. De Cian[12], J.M. De Miranda[1], L. De Paula[2], M. De Serio[14,d], P. De Simone[19], C.-T. Dean[52], D. Decamp[4], M. Deckenhoff[10], L. Del Buono[8], M. Demmer[10], D. Derkach[67], O. Deschamps[5], F. Dettori[39], B. Dey[22], A. Di Canto[39], H. Dijkstra[39], F. Dordei[39], M. Dorigo[40], A. Dosil Suárez[38], A. Dovbnya[44], K. Dreimanis[53], L. Dufour[42], G. Dujany[55], K. Dungs[39], P. Durante[39], R. Dzhelyadin[36], A. Dziurda[39], A. Dzyuba[31], N. Déléage[4], S. Easo[50], U. Egede[54], V. Egorychev[32], S. Eidelman[35], S. Eisenhardt[51], U. Eitschberger[10], R. Ekelhof[10], L. Eklund[52], Ch. Elsasser[41], S. Ely[60], S. Esen[12], H.M. Evans[48], T. Evans[56], A. Falabella[15], N. Farley[46], S. Farry[53], R. Fay[53], D. Fazzini[21,i], D. Ferguson[51], V. Fernandez Albor[38], F. Ferrari[15,39], F. Ferreira Rodrigues[1], M. Ferro-Luzzi[39], S. Filippov[34], R.A. Fini[14], M. Fiore[17,g], M. Fiorini[17,g], M. Firlej[28], C. Fitzpatrick[40], T. Fiutowski[28], F. Fleuret[7,b], K. Fohl[39], M. Fontana[16], F. Fontanelli[20,h], D.C. Forshaw[60], R. Forty[39], V. Franco Lima[53], M. Frank[39], C. Frei[39], J. Fu[22,q], E. Furfaro[25,j], C. Färber[39], A. Gallas Torreira[38], D. Galli[15,e], S. Gallorini[23], S. Gambetta[51], M. Gandelman[2], P. Gandini[56], Y. Gao[3], J. García Pardiñas[38], J. Garra Tico[48], L. Garrido[37], P.J. Garsed[48], D. Gascon[37], C. Gaspar[39], L. Gavardi[10], G. Gazzoni[5], D. Gerick[12], E. Gersabeck[12], M. Gersabeck[55], T. Gershon[49], Ph. Ghez[4], S. Gianì[40], V. Gibson[48], E. Gillies[51], O.G. Girard[40], L. Giubega[30], K. Gizdov[51], V.V. Gligorov[8], D. Golubkov[32], A. Golutvin[54,39], A. Gomes[1,a], I.V. Gorelov[33], C. Gotti[21,i], M. Grabalosa Gándara[5], R. Graciani Diaz[37], L.A. Granado Cardoso[39], E. Graugés[37], E. Graverini[41], G. Graziani[18], A. Grecu[30], P. Griffith[46], L. Grillo[21], B.R. Gruberg Cazon[56], O. Grünberg[65], E. Gushchin[34], Yu. Guz[36], T. Gys[39], C. Göbel[61], T. Hadavizadeh[56], C. Hadjivasiliou[5], G. Haefeli[40], C. Haen[39], S.C. Haines[48], S. Hall[54], B. Hamilton[59], X. Han[12], S. Hansmann-Menzemer[12], N. Harnew[56], S.T. Harnew[47],

J. Harrison[55], M. Hatch[39], J. He[62], T. Head[40], A. Heister[9], K. Hennessy[53], P. Henrard[5], L. Henry[8], J.A. Hernando Morata[38], E. van Herwijnen[39], M. Heß[65], A. Hicheur[2], D. Hill[56], C. Hombach[55], W. Hulsbergen[42], T. Humair[54], M. Hushchyn[67], N. Hussain[56], D. Hutchcroft[53], M. Idzik[28], P. Ilten[57], R. Jacobsson[39], A. Jaeger[12], J. Jalocha[56], E. Jans[42], A. Jawahery[59], M. John[56], D. Johnson[39], C.R. Jones[48], C. Joram[39], B. Jost[39], N. Jurik[60], S. Kandybei[44], W. Kanso[6], M. Karacson[39], J.M. Kariuki[47], S. Karodia[52], M. Kecke[12], M. Kelsey[60], I.R. Kenyon[46], M. Kenzie[39], T. Ketel[43], E. Khairullin[67], B. Khanji[21,39,i], C. Khurewathanakul[40], T. Kirn[9], S. Klaver[55], K. Klimaszewski[29], S. Koliiev[45], M. Kolpin[12], I. Komarov[40], R.F. Koopman[43], P. Koppenburg[42], A. Kozachuk[33], M. Kozeiha[5], L. Kravchuk[34], K. Kreplin[12], M. Kreps[49], P. Krokovny[35], F. Kruse[10], W. Krzemien[29], W. Kucewicz[27,l], M. Kucharczyk[27], V. Kudryavtsev[35], A.K. Kuonen[40], K. Kurek[29], T. Kvaratskheliya[32,39], D. Lacarrere[39], G. Lafferty[55,39], A. Lai[16], D. Lambert[51], G. Lanfranchi[19], C. Langenbruch[9], B. Langhans[39], T. Latham[49], C. Lazzeroni[46], R. Le Gac[6], J. van Leerdam[42], J.-P. Lees[4], A. Leflat[33,39], J. Lefrançois[7], R. Lefèvre[5], F. Lemaitre[39], E. Lemos Cid[38], O. Leroy[6], T. Lesiak[27], B. Leverington[12], Y. Li[7], T. Likhomanenko[67,66], R. Lindner[39], C. Linn[39], F. Lionetto[41], B. Liu[16], X. Liu[3], D. Loh[49], I. Longstaff[52], J.H. Lopes[2], D. Lucchesi[23,o], M. Lucio Martinez[38], H. Luo[51], A. Lupato[23], E. Luppi[17,g], O. Lupton[56], A. Lusiani[24], X. Lyu[62], F. Machefert[7], F. Maciuc[30], O. Maev[31], K. Maguire[55], S. Malde[56], A. Malinin[66], T. Maltsev[35], G. Manca[7], G. Mancinelli[6], P. Manning[60], J. Maratas[5,v], J.F. Marchand[4], U. Marconi[15], C. Marin Benito[37], P. Marino[24,t], J. Marks[12], G. Martellotti[26], M. Martin[6], M. Martinelli[40], D. Martinez Santos[38], F. Martinez Vidal[68], D. Martins Tostes[2], L.M. Massacrier[7], A. Massafferri[1], R. Matev[39], A. Mathad[49], Z. Mathe[39], C. Matteuzzi[21], A. Mauri[41], B. Maurin[40], A. Mazurov[46], M. McCann[54], J. McCarthy[46], A. McNab[55], R. McNulty[13], B. Meadows[58], F. Meier[10], M. Meissner[12], D. Melnychuk[29], M. Merk[42], A. Merli[22,q], E. Michielin[23], D.A. Milanes[64], M.-N. Minard[4], D.S. Mitzel[12], J. Molina Rodriguez[61], I.A. Monroy[64], S. Monteil[5], M. Morandin[23], P. Morawski[28], A. Mordà[6], M.J. Morello[24,t], J. Moron[28], A.B. Morris[51], R. Mountain[60], F. Muheim[51], M. Mulder[42], M. Mussini[15], D. Müller[55], J. Müller[10], K. Müller[41], V. Müller[10], P. Naik[47], T. Nakada[40], R. Nandakumar[50], A. Nandi[56], I. Nasteva[2], M. Needham[51], N. Neri[22], S. Neubert[12], N. Neufeld[39], M. Neuner[12], A.D. Nguyen[40], C. Nguyen-Mau[40,n], S. Nieswand[9], R. Niet[10], N. Nikitin[33], T. Nikodem[12], A. Novoselov[36], D.P. O'Hanlon[49], A. Oblakowska-Mucha[28], V. Obraztsov[36], S. Ogilvy[19], R. Oldeman[48], C.J.G. Onderwater[69], J.M. Otalora Goicochea[2], A. Otto[39], P. Owen[41], A. Oyanguren[68], P.R. Pais[40], A. Palano[14,d], F. Palombo[22,q], M. Palutan[19], J. Panman[39], A. Papanestis[50], M. Pappagallo[14,d], L.L. Pappalardo[17,g], C. Pappenheimer[58], W. Parker[59], C. Parkes[55], G. Passaleva[18], A. Pastore[14,d], G.D. Patel[53], M. Patel[54], C. Patrignani[15,e], A. Pearce[55,50], A. Pellegrino[42], G. Penso[26,k], M. Pepe Altarelli[39], S. Perazzini[39], P. Perret[5], L. Pescatore[46], K. Petridis[47], A. Petrolini[20,h], A. Petrov[66], M. Petruzzo[22,q], E. Picatoste Olloqui[37], B. Pietrzyk[4], M. Pikies[27], D. Pinci[26], A. Pistone[20], A. Piucci[12], S. Playfer[51], M. Plo Casasus[38], T. Poikela[39], F. Polci[8], A. Poluektov[49,35], I. Polyakov[60], E. Polycarpo[2], G.J. Pomery[47], A. Popov[36], D. Popov[11,39], B. Popovici[30], C. Potterat[2], E. Price[47], J.D. Price[53], J. Prisciandaro[38], A. Pritchard[53], C. Prouve[47], V. Pugatch[45], A. Puig Navarro[40], G. Punzi[24,p], W. Qian[56], R. Quagliani[7,47], B. Rachwal[27], J.H. Rademacker[47], M. Rama[24], M. Ramos Pernas[38], M.S. Rangel[2], I. Raniuk[44], G. Raven[43], F. Redi[54], S. Reichert[10], A.C. dos Reis[1], C. Remon Alepuz[68], V. Renaudin[7], S. Ricciardi[50], S. Richards[47], M. Rihl[39], K. Rinnert[53,39], V. Rives Molina[37], P. Robbe[7,39], A.B. Rodrigues[1], E. Rodrigues[58], J.A. Rodriguez Lopez[64], P. Rodriguez Perez[55], A. Rogozhnikov[67], S. Roiser[39], V. Romanovskiy[36], A. Romero Vidal[38], J.W. Ronayne[13], M. Rotondo[23], M.S. Rudolph[60], T. Ruf[39], P. Ruiz Valls[68], J.J. Saborido Silva[38], E. Sadykhov[32], N. Sagidova[31], B. Saitta[16,f], V. Salustino Guimaraes[2], C. Sanchez Mayordomo[68], B. Sanmartin Sedes[38], R. Santacesaria[26], C. Santamarina Rios[38], M. Santimaria[19], E. Santovetti[25,j], A. Sarti[19,k], C. Satriano[26,s],

A. Satta[25], D.M. Saunders[47], D. Savrina[32,33], S. Schael[9], M. Schellenberg[10], M. Schiller[39], H. Schindler[39], M. Schlupp[10], M. Schmelling[11], T. Schmelzer[10], B. Schmidt[39], O. Schneider[40], A. Schopper[39], K. Schubert[10], M. Schubiger[40], M.-H. Schune[7], R. Schwemmer[39], B. Sciascia[19], A. Sciubba[26,k], A. Semennikov[32], A. Sergi[46], N. Serra[41], J. Serrano[6], L. Sestini[23], P. Seyfert[21], M. Shapkin[36], I. Shapoval[17,44,g], Y. Shcheglov[31], T. Shears[53], L. Shekhtman[35], V. Shevchenko[66], A. Shires[10], B.G. Siddi[17], R. Silva Coutinho[41], L. Silva de Oliveira[2], G. Simi[23,o], S. Simone[14,d], M. Sirendi[48], N. Skidmore[47], T. Skwarnicki[60], E. Smith[54], I.T. Smith[51], J. Smith[48], M. Smith[55], H. Snoek[42], M.D. Sokoloff[58], F.J.P. Soler[52], D. Souza[47], B. Souza De Paula[2], B. Spaan[10], P. Spradlin[52], S. Sridharan[39], F. Stagni[39], M. Stahl[12], S. Stahl[39], P. Stefko[40], S. Stefkova[54], O. Steinkamp[41], O. Stenyakin[36], S. Stevenson[56], S. Stoica[30], S. Stone[60], B. Storaci[41], S. Stracka[24,t], M. Straticiuc[30], U. Straumann[41], L. Sun[58], W. Sutcliffe[54], K. Swientek[28], V. Syropoulos[43], M. Szczekowski[29], T. Szumlak[28], S. T'Jampens[4], A. Tayduganov[6], T. Tekampe[10], G. Tellarini[17,g], F. Teubert[39], C. Thomas[56], E. Thomas[39], J. van Tilburg[42], V. Tisserand[4], M. Tobin[40], S. Tolk[48], L. Tomassetti[17,g], D. Tonelli[39], S. Topp-Joergensen[56], F. Toriello[60], E. Tournefier[4], S. Tourneur[40], K. Trabelsi[40], M. Traill[52], M.T. Tran[40], M. Tresch[41], A. Trisovic[39], A. Tsaregorodtsev[6], P. Tsopelas[42], A. Tully[48], N. Tuning[42], A. Ukleja[29], A. Ustyuzhanin[67,66], U. Uwer[12], C. Vacca[16,39,f], V. Vagnoni[15,39], S. Valat[39], G. Valenti[15], A. Vallier[7], R. Vazquez Gomez[19], P. Vazquez Regueiro[38], S. Vecchi[17], M. van Veghel[42], J.J. Velthuis[47], M. Veltri[18,r], G. Veneziano[40], A. Venkateswaran[60], M. Vernet[5], M. Vesterinen[12], B. Viaud[7], D. Vieira[1], M. Vieites Diaz[38], X. Vilasis-Cardona[37,m], V. Volkov[33], A. Vollhardt[41], B. Voneki[39], D. Voong[47], A. Vorobyev[31], V. Vorobyev[35], C. Voß[65], J.A. de Vries[42], C. Vázquez Sierra[38], R. Waldi[65], C. Wallace[49], R. Wallace[13], J. Walsh[24], J. Wang[60], D.R. Ward[48], H.M. Wark[53], N.K. Watson[46], D. Websdale[54], A. Weiden[41], M. Whitehead[39], J. Wicht[49], G. Wilkinson[56,39], M. Wilkinson[60], M. Williams[39], M.P. Williams[46], M. Williams[57], T. Williams[46], F.F. Wilson[50], J. Wimberley[59], J. Wishahi[10], W. Wislicki[29], M. Witek[27], G. Wormser[7], S.A. Wotton[48], K. Wraight[52], S. Wright[48], K. Wyllie[39], Y. Xie[63], Z. Xing[60], Z. Xu[40], Z. Yang[3], H. Yin[63], J. Yu[63], X. Yuan[35], O. Yushchenko[36], M. Zangoli[15], K.A. Zarebski[46], M. Zavertyaev[11,c], L. Zhang[3], Y. Zhang[7], Y. Zhang[62], A. Zhelezov[12], Y. Zheng[62], A. Zhokhov[32], V. Zhukov[9], S. Zucchelli[15].

[1]*Centro Brasileiro de Pesquisas Físicas (CBPF), Rio de Janeiro, Brazil*
[2]*Universidade Federal do Rio de Janeiro (UFRJ), Rio de Janeiro, Brazil*
[3]*Center for High Energy Physics, Tsinghua University, Beijing, China*
[4]*LAPP, Université Savoie Mont-Blanc, CNRS/IN2P3, Annecy-Le-Vieux, France*
[5]*Clermont Université, Université Blaise Pascal, CNRS/IN2P3, LPC, Clermont-Ferrand, France*
[6]*CPPM, Aix-Marseille Université, CNRS/IN2P3, Marseille, France*
[7]*LAL, Université Paris-Sud, CNRS/IN2P3, Orsay, France*
[8]*LPNHE, Université Pierre et Marie Curie, Université Paris Diderot, CNRS/IN2P3, Paris, France*
[9]*I. Physikalisches Institut, RWTH Aachen University, Aachen, Germany*
[10]*Fakultät Physik, Technische Universität Dortmund, Dortmund, Germany*
[11]*Max-Planck-Institut für Kernphysik (MPIK), Heidelberg, Germany*
[12]*Physikalisches Institut, Ruprecht-Karls-Universität Heidelberg, Heidelberg, Germany*
[13]*School of Physics, University College Dublin, Dublin, Ireland*
[14]*Sezione INFN di Bari, Bari, Italy*
[15]*Sezione INFN di Bologna, Bologna, Italy*
[16]*Sezione INFN di Cagliari, Cagliari, Italy*
[17]*Sezione INFN di Ferrara, Ferrara, Italy*
[18]*Sezione INFN di Firenze, Firenze, Italy*
[19]*Laboratori Nazionali dell'INFN di Frascati, Frascati, Italy*
[20]*Sezione INFN di Genova, Genova, Italy*
[21]*Sezione INFN di Milano Bicocca, Milano, Italy*
[22]*Sezione INFN di Milano, Milano, Italy*
[23]*Sezione INFN di Padova, Padova, Italy*

[24]*Sezione INFN di Pisa, Pisa, Italy*
[25]*Sezione INFN di Roma Tor Vergata, Roma, Italy*
[26]*Sezione INFN di Roma La Sapienza, Roma, Italy*
[27]*Henryk Niewodniczanski Institute of Nuclear Physics Polish Academy of Sciences, Kraków, Poland*
[28]*AGH - University of Science and Technology, Faculty of Physics and Applied Computer Science, Kraków, Poland*
[29]*National Center for Nuclear Research (NCBJ), Warsaw, Poland*
[30]*Horia Hulubei National Institute of Physics and Nuclear Engineering, Bucharest-Magurele, Romania*
[31]*Petersburg Nuclear Physics Institute (PNPI), Gatchina, Russia*
[32]*Institute of Theoretical and Experimental Physics (ITEP), Moscow, Russia*
[33]*Institute of Nuclear Physics, Moscow State University (SINP MSU), Moscow, Russia*
[34]*Institute for Nuclear Research of the Russian Academy of Sciences (INR RAN), Moscow, Russia*
[35]*Budker Institute of Nuclear Physics (SB RAS) and Novosibirsk State University, Novosibirsk, Russia*
[36]*Institute for High Energy Physics (IHEP), Protvino, Russia*
[37]*ICCUB, Universitat de Barcelona, Barcelona, Spain*
[38]*Universidad de Santiago de Compostela, Santiago de Compostela, Spain*
[39]*European Organization for Nuclear Research (CERN), Geneva, Switzerland*
[40]*Ecole Polytechnique Fédérale de Lausanne (EPFL), Lausanne, Switzerland*
[41]*Physik-Institut, Universität Zürich, Zürich, Switzerland*
[42]*Nikhef National Institute for Subatomic Physics, Amsterdam, The Netherlands*
[43]*Nikhef National Institute for Subatomic Physics and VU University Amsterdam, Amsterdam, The Netherlands*
[44]*NSC Kharkiv Institute of Physics and Technology (NSC KIPT), Kharkiv, Ukraine*
[45]*Institute for Nuclear Research of the National Academy of Sciences (KINR), Kyiv, Ukraine*
[46]*University of Birmingham, Birmingham, United Kingdom*
[47]*H.H. Wills Physics Laboratory, University of Bristol, Bristol, United Kingdom*
[48]*Cavendish Laboratory, University of Cambridge, Cambridge, United Kingdom*
[49]*Department of Physics, University of Warwick, Coventry, United Kingdom*
[50]*STFC Rutherford Appleton Laboratory, Didcot, United Kingdom*
[51]*School of Physics and Astronomy, University of Edinburgh, Edinburgh, United Kingdom*
[52]*School of Physics and Astronomy, University of Glasgow, Glasgow, United Kingdom*
[53]*Oliver Lodge Laboratory, University of Liverpool, Liverpool, United Kingdom*
[54]*Imperial College London, London, United Kingdom*
[55]*School of Physics and Astronomy, University of Manchester, Manchester, United Kingdom*
[56]*Department of Physics, University of Oxford, Oxford, United Kingdom*
[57]*Massachusetts Institute of Technology, Cambridge, MA, United States*
[58]*University of Cincinnati, Cincinnati, OH, United States*
[59]*University of Maryland, College Park, MD, United States*
[60]*Syracuse University, Syracuse, NY, United States*
[61]*Pontifícia Universidade Católica do Rio de Janeiro (PUC-Rio), Rio de Janeiro, Brazil, associated to* [2]
[62]*University of Chinese Academy of Sciences, Beijing, China, associated to* [3]
[63]*Institute of Particle Physics, Central China Normal University, Wuhan, Hubei, China, associated to* [3]
[64]*Departamento de Fisica , Universidad Nacional de Colombia, Bogota, Colombia, associated to* [8]
[65]*Institut für Physik, Universität Rostock, Rostock, Germany, associated to* [12]
[66]*National Research Centre Kurchatov Institute, Moscow, Russia, associated to* [32]
[67]*Yandex School of Data Analysis, Moscow, Russia, associated to* [32]
[68]*Instituto de Fisica Corpuscular (IFIC), Universitat de Valencia-CSIC, Valencia, Spain, associated to* [37]
[69]*Van Swinderen Institute, University of Groningen, Groningen, The Netherlands, associated to* [42]

[a]*Universidade Federal do Triângulo Mineiro (UFTM), Uberaba-MG, Brazil*
[b]*Laboratoire Leprince-Ringuet, Palaiseau, France*
[c]*P.N. Lebedev Physical Institute, Russian Academy of Science (LPI RAS), Moscow, Russia*
[d]*Università di Bari, Bari, Italy*
[e]*Università di Bologna, Bologna, Italy*
[f]*Università di Cagliari, Cagliari, Italy*
[g]*Università di Ferrara, Ferrara, Italy*
[h]*Università di Genova, Genova, Italy*

[i] *Università di Milano Bicocca, Milano, Italy*
[j] *Università di Roma Tor Vergata, Roma, Italy*
[k] *Università di Roma La Sapienza, Roma, Italy*
[l] *AGH - University of Science and Technology, Faculty of Computer Science, Electronics and Telecommunications, Kraków, Poland*
[m] *LIFAELS, La Salle, Universitat Ramon Llull, Barcelona, Spain*
[n] *Hanoi University of Science, Hanoi, Viet Nam*
[o] *Università di Padova, Padova, Italy*
[p] *Università di Pisa, Pisa, Italy*
[q] *Università degli Studi di Milano, Milano, Italy*
[r] *Università di Urbino, Urbino, Italy*
[s] *Università della Basilicata, Potenza, Italy*
[t] *Scuola Normale Superiore, Pisa, Italy*
[u] *Università di Modena e Reggio Emilia, Modena, Italy*
[v] *Iligan Institute of Technology (IIT), Iligan, Philippines*